GeoVirtual 2020 September 14-16 Resilience and Innovation

Viscous (time-dependent) behaviour of saturated clay in consolidated undrained triaxial compression

Chee K. Wong[1], Biao Li[2] & Ron C.K. Wong[3]
[1]Research Associate, Department of Civil Engineering – University of Calgary, Calgary, AB, Canada
[2]Assistant Professor, Department of Building, Civil, and Environmental Engineering – Concordia University, Montreal, QC, Canada
[3]Professor, Department of Civil Engineering – University of Calgary, Calgary, AB, Canada

ABSTRACT
The strength-deformation-pore pressure characteristics of saturated clay under consolidated undrained (CU) triaxial compression are highly dependent on the applied strain rate. An increase in strain rate causes an increase in undrained peak strength, reflecting the viscous plastic behaviour of the material. Based on the theory of critical state plasticity, the increase in undrained peak strength due to the increase in strain rate could be modelled by an apparent increase in overconsolidation pressure or ratio (OCR). Since the OCR controls the loci of the yield surface or function, the yield surface becomes non-stationary (dynamic) and rate-dependent. Based on the strain rate dependency among the undrained peak strength, OCR and dynamic yield surface, this paper develops an interpretation technique to correlate the undrained strength parameters measured in CU tests with the Hvorslev drained strength parameters. The drained strength parameters are rate-dependent (viscous) cohesion and rate-independent (intrinsic) true friction angle. Data of CU tests on resedimented Boston blue clay will be processed and analyzed using the proposed interpretation technique. Correlation analysis of test results reveals that the Hvorslev cohesion is function of strain rate and void ratio (or consolidation history).

RÉSUMÉ
Les caractéristiques résistance-déformation-pression interstitielle de l'argile saturée sous compression triaxiale consolidée non drainée (CU) dépendent fortement du taux de déformation appliqué. Une augmentation de la vitesse de déformation entraîne une augmentation de la résistance maximale non drainée, reflétant le comportement plastique visqueux du matériau. Sur la base de la théorie de la plasticité de l'état critique, l'augmentation de la résistance crête non drainée due à l'augmentation de la vitesse de déformation pourrait être modélisée par une augmentation apparente de la pression ou du rapport de surconsolidation (OCR). Étant donné que l'OCR contrôle les loci de la surface ou de la fonction de rendement, la surface de rendement devient non stationnaire (dynamique) et dépendante du débit. Basé sur la dépendance du taux de déformation entre la résistance maximale non drainée, l'OCR et la surface de rendement dynamique, cet article développe une technique d'interprétation pour corréler les paramètres de résistance non drainés mesurés dans les tests CU avec les paramètres de résistance drainée Hvorslev. Les paramètres de résistance drainée sont la cohésion dépendante du taux (visqueux) et l'angle de frottement réel (intrinsèque) indépendant du taux. Les données des tests d'UC sur l'argile bleue de Boston resédimentée seront traitées et analysées à l'aide de la technique d'interprétation proposée. L'analyse de corrélation des résultats des tests révèle que la cohésion Hvorslev est fonction de la vitesse de déformation et du rapport des vides (ou historique de consolidation).

1 INTRODUCTION

Rate-dependent changes in soil properties are important in geotechnical problems in which the variation of soil displacement rate and magnitude is significant. They include: soil-pipe interaction in moving slopes, landslides in natural and excavated slopes, deformation of earth structures, and foundation settlement in soft clay. The soil displacement (strain) rate not only induces excess pore pressure, but also has an effect on the shear strength in saturated soils. Soil drained strength parameters such as cohesion and effective friction angle are recommended to be used in effective stress analysis of stability of geotechnical structures. These drained shear strength parameters are commonly assumed to be independent of strain rate. Ideally, consolidated drained triaxial compression (CD) tests should be conducted to study the strain-rate or viscous behaviour of saturated

clay. In drained tests, the effective stress path is well-defined and the deformation is mainly due to the change in shear stress as no or insignificant excess pore pressure is induced. However, the strain rate may be as slow as 0.1%/h for low-permeability clay to maintain the drained condition, and the test duration is very long. Thus, the effect of strain rate on the stress-strain-strength behaviour of saturated clays has been studied extensively using consolidated undrained triaxial compression (CU) tests (e.g., Taylor 1943; Casagrande and Wilson 1951; Richardson and Whitman 1963; Graham et al. 1983; Lefebvre and Pfendler 1996; Sheahan et al. 1996; Vaid and Campanella 1997; Zhu and Yin 2000). One of the advantages of CU tests is that any strain rate can be applied to the test specimen under undrained condition. In addition, the effective stress path can be used to determine the shape of the yield surface as it may intersect and travel along part of the yield surface at constant void ratio. Tests with high strain rates would induce excess pore pressure in the soil specimen, and the stress-strain response is dependent on the drainage condition. The total soil deformation is due to not only the change in effective stress, but also the strain rate-dependent (viscous) effect. It is challenging to decouple the two mechanisms, which is quite comparable to decoupling of consolidation and creep deformations occurred simultaneously in 1D compression test (Wong et al. 2018). The objectives of this paper are to analyze data from CU tests under varying strain rates, and to delineate which parameters identified in the tests are uniquely intrinsic and independent of strain rate, and which parameters are rate-dependent. The first part of the paper reviews theoretical and empirical correlations among undrained shear strength, overconsolidation ratio (OCR) and strain rate in clay. The second part proposes a mathematical framework and an interpretation technique to determine rate-dependent drained shear strength parameters of clay from undrained response observed in CU tests. Experimental evidences are provided from undrained shear response of resedimented Boston blue clay (BBC) in anisotropically consolidated undrained triaxial compression tests (CK_0UC) tests, along with concluding remarks.

2 BACKGROUND

2.1 State- (stress history-) dependent undrained shear strength

Undrained shear strength s_u may be used in total stress analysis to investigate the short-term failure state of geotechnical structures. For clay under normal consolidation, the undrained shear strength of the material can be theoretically related to its material constants defined in the critical state model (Mayne 1980; Wroth 1984):

$$\frac{s_u}{p_i} = \frac{M}{2} r^{-\Lambda_o} \text{ for NC clay} \quad [1]$$

where s_u is the undrained shear strength; p_i is the isotropic consolidation stress; M is the slope of the critical state line ($M = \frac{6 \sin \phi_{cs}}{(3 - sin\phi_{cs})}$); ϕ_{cs} is the critical state angle; is equal the base of natural logarithm or 2; Λ_o is a function of coefficients of normal consolidation and rebound curves. For overconsolidated (OC) clay, [1] becomes:

$$\frac{s_u}{p_i} = S(R_0)^{\Lambda_o} \text{ for OC clay} \quad [2]$$

where S = the p_i- normalized undrained shear strength for NC clay ($S = \frac{M}{2}(r)^{-\Lambda_o}$); R_0 = preconsolidation ratio of the maximum isotropic consolidation stress to the current isotropic consolidation stress.

According to the critical state soil mechanics, s_u in [1] and [2] represent the undrained shear strengths for NC and OC clay at their critical (failure) states, respectively. Figs. 1 and 2 are used to illustrate the effect of the state or stress history on their undrained responses. In Fig. 1, consider two specimens, NC and OC with a same void ratio. Upon CU loading, the NC and OC specimens undergo the 1-2 and 3-4-5 stress paths, respectively, and fail at the same critical void ratio or state (states '2' and '5') with the same value of undrained shear strength. This implies than s_u is not a fundamental soil property as it depends on its initial void ratio or state. From Fig. 1b, the OC specimen may display a peak q-stress (state '4') followed by strain softening (path 4-5) to the critical state (state '5'). The peak p_i- normalized undrained shear strength of OC soil may be given as (Budhu 2011; p. 351):

$$\frac{s_u}{p_i} = \frac{M}{2}(R_0 - 1)^{0.5};\ R_0 > 1 \quad [3]$$

The OC specimen could not go beyond its limiting state, i.e., the states beyond the elliptical yield surface ('a'-'c') are inadmissible.

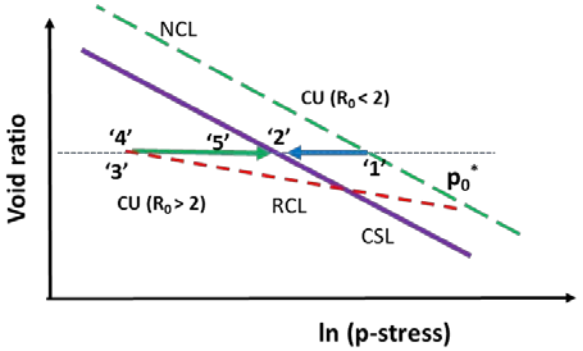

(a)

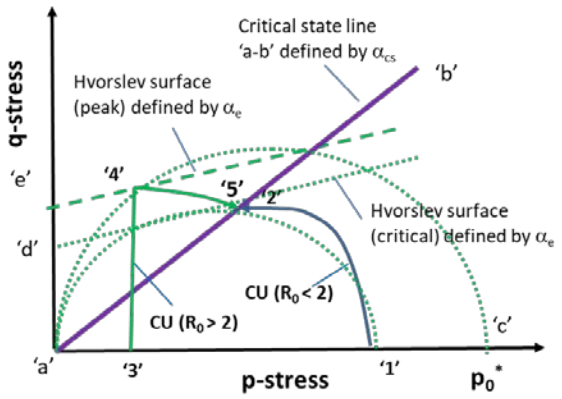

(b)

Fig. 1 Stress paths for NC and OC specimens with same void ratio in CU tests (a) e-p plot and (b) p-q plot

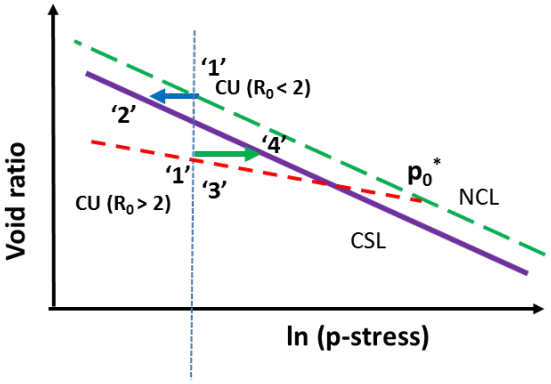

(a)

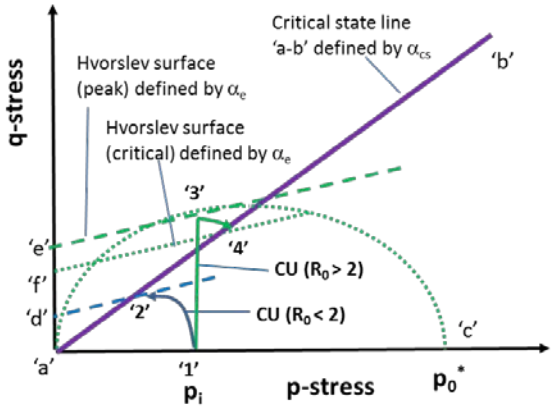

(b)

Fig. 2 Stress paths for NC and OC specimens under same isotropic consolidation pressure in CU tests (a) e-p plot and (b) p-q plot

The critical state model assumes that the yield surfaces are elliptical, and predicts no post-peak strain softening for NC soil in CU test (for a symmetrical elliptical yield surface at a given constant void ratio under undrained condition, the p-stress at critical state is half of the p-stress at consolidation). However, peak behavior may be also observed in some NC soils under CU loading because the yield surface may deviate from the elliptical configuration idealized in the critical state model. This peak state lies on the yield surface well below the critical state line in p-q plot, and the specimen will reach its failure at the critical state upon further loading. Thus, the peak stress states observed in NC and OC soils are distinctly different behaviours.

Fig. 2 compares the stress paths for NC and OC specimens under a same consolidation stress subject to CU loading in e-p and p-q plots. The undrained shear strength of OC specimen is much higher than that of NC specimen due to higher R_0 reflected in [2].

Ladd and Foot (1974) used the SHANSEP (stress history and normalized soil engineering properties) method to develop an empirical correlation with experimental data, which is similar to [2]:

$$\frac{s_u}{\sigma'_{vc}} = S(OCR)^m \qquad [4]$$

where *S* and m are constants depending on soil type; σ'_{vc} = current vertical consolidation stress; OCR = overconsolidation ratio of current vertical consolidation stress to maximum vertical consolidation stress. For isotropic consolidation, $OCR = R_0$.

2.2 Rate-dependent undrained shear strength

In addition to the effect of stress history, the time-dependent (viscous) or rate effect also affects the undrained shear strength, i.e., the undrained shear strength increases with increasing strain rate. Based on experimental data, Kulhawy and Mayne (1990) proposed a semi-logarithmic law to characterize the rate effect for cohesive soils from different sources:

$$\frac{s_u}{s_{u0}} = 1 + m_{KM} \log(\frac{\dot{\varepsilon}}{\dot{\varepsilon}_0}) \qquad [5]$$

where s_{u0} = the undrained shear strength at reference strain rate $\dot{\varepsilon}_0$; $\dot{\varepsilon}$ = strain rate; m_{KM} = correlation parameter. For $\dot{\varepsilon}_0$ = 1%/hr, m_{KM} = 0.1 based on regression analysis of experimental data (Kulhawy and Mayne 1990).

Graham et al. (1983) adopted the semi-logarithmic relationship of [5] and normalized s_u by σ'_{vc}:

$$\frac{s_u}{\sigma'_{vc}} = \frac{s_{u0}}{\sigma'_{vc}} + m_{vc} \log(\frac{\dot{\varepsilon}}{\dot{\varepsilon}_0}) \qquad [6]$$

where $m_{vc} = \frac{s_{u0}}{\sigma'_{vc}} m_{KM}$.

Other than using the semi-logarithmic relationship between the undrained shear strength and strain rate, log-log or power law has been used to curve fit test data (Soga and Mitchell 1996):

$$\log s_u = \log s_{u0} + m_{SM} \log(\frac{\dot{\varepsilon}}{\dot{\varepsilon}_0}) \qquad [7]$$

where $m_{SM} = \frac{\log\left(\frac{s_u}{s_{u0}}\right)}{\log\left(\frac{\dot{\varepsilon}}{\dot{\varepsilon}_o}\right)}$. Comparison between m_{KM} in [5] and m_{SM} in [7] by equating the term of $\log\left(\frac{\dot{\varepsilon}}{\dot{\varepsilon}_o}\right)$ shows:

$$\frac{m_{SM}}{m_{kM}} = \frac{\log\left(\frac{s_u}{s_{u0}}\right)}{\Delta\left(\frac{s_u}{s_{u0}}\right)} \quad [8]$$

For $\frac{s_u}{s_{u0}}$ = 1-1.25, $m_{SM} \approx 0.39 m_{KM}$ as illustrated in Fig. 3.

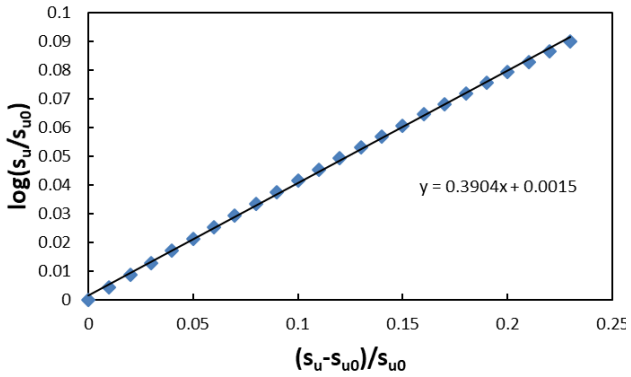

Fig. 3. Comparison between log-log (power) and semi-logarithmic laws of undrained shear strength and strain rate

2.3 State- and rate- dependent undrained shear strength

The rate dependency relationships proposed by Kulhawy and Mayne (1980) and others are not specific to NC or OC soils. We postulate the normalized undrained shear strength *S* in [3] follows the semi-logarithmic law (Zhu and Yin 2001). Then, [3] becomes:

$$\frac{s_u}{\sigma'_{vc}} = \left[\frac{s_{u0}}{\sigma'_{vc}}_{OCR=1} + m_{vc}\log\left(\frac{\dot{\varepsilon}}{\dot{\varepsilon}_0}\right)\right](OCR)^m \quad [9]$$

The undrained shear strength criteria of [1] – [9] define the failure state in terms of total stresses, and are insufficient to characterize the failure state for effective stress analysis. To define the effective stresses at failure state, the undrained shear strength coupled with the induced pore pressure at failure state, u_f or minor principal effective stress, σ'_{3f} must be measured in the CU tests.

3 PROPOSED INTERPRETATION METHOD FOR STATE- AND RATE- DEPENDENT DRAINED STRENGTH PRAMETERS OF SATURATED CLAY

Constitutive models have been developed for rate sensitive plastic materials and clays (e.g., Perzyna 1963; Kutter and Sathialingam 1992; Nakai et al. 2011). Most of these models are built upon the classical plasticity theory. A rate-independent yield surface is defined to represent the inviscid (or static) yield condition for the initiation of plastic deformation. For simplicity, only time-independent deformation occurs in the elastic regime, and time-dependent or viscous deformation occurs along with the plastic strain. For accounting the rate-dependent effect, the material's state is allowed to go beyond the static yield surface (SYS), i.e., the static yield surface is allowed to expand or harden to a new rate-dependent (dynamic) yield surface (DYS). The strain rate for SYS may be as low as 0.02%/h (Sheahan 1995). Elastic strains are assumed to occur inside the current DYS whereas the viscoplastic strains are assumed to develop along the current DYS. This generalized framework will be used to understand the undrained responses of normally consolidated (NC) and overconsolidated (OC) clays under triaxial compression and to extract intrinsic rate-independent and rate-dependent material properties. Evaluation of constitutive models is beyond the scope of this study.

Consider the undrained response of normally consolidated (NC) clay under triaxial compression in a p-q stress plot of Fig. 4 ($q = \frac{1}{2}(\sigma'_1 - \sigma'_3)$ and $p = \frac{1}{2}(\sigma'_1 + \sigma'_3)$ where σ'_1 and σ'_3 are major and minor principal effective stresses, respectively). Two clay specimens are allowed to hydrostatically consolidate to point '1' below a common static yield surface, and sheared in undrained condition at two different strain rates. Undrained stress path '1-2' has a lower strain rate than undrained stress path '1-3. Curves 'a-c' and 'a-d correspond to the loci of parts of hypothetical dynamic yield surfaces (DYS_1 and DYS_2) at a constant void ratio or undrained condition (parts of DYSs above the critical state line 'a-b' were not shown in the figure for clarity). Two specimens fail at different states along the critical state line 'a-b'. The undrained responses of the two NC specimens are different mainly due to the difference in strain rates as quantified by Katti et al. (2003). An increase in strain rate causes an apparent increase in OCR along with an expanded DYS (the SYS grows to surfaces 'a-c' and 'a-d' with increasing strain rate), and thus, an increase in undrained peak strength at the critical states '2' and '3'.

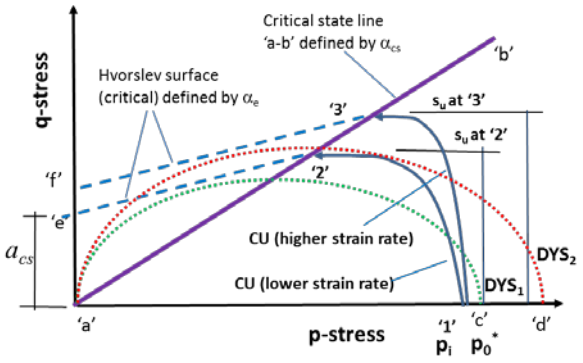

Fig. 4. Undrained behavior of normally or lightly overconsolidated specimens with different strain rates

In Fig. 4, the NC specimens fail at states along the critical state line defined by the angle α_{cs} in the p-q plot. It appears that the drained shear strength of NC clay is

independent of strain rate if this critical state angle is used in defining the drained (effective stress) failure envelope of the material. To account for the rate-dependent shear strength observed in CU tests, we propose to use Hvorslev failure envelope to define the rate-dependent failure state on the critical state (states '2' and '3' in Fig. 4) as follows:

$$q = a_{cs}(e, \dot{\varepsilon}) + p\tan(\alpha_e) \quad [10]$$

where $a_{cs}(e, \dot{\varepsilon})$= Hvorslev cohesion in p-q plot depending on void ratio *e* and strain rate $\dot{\varepsilon}$; the subscript *cs* refers to critical state; α_e = Hvorslev friction angle. Equation [6] can be expressed in the conventional Mohr-Coulomb envelope of:

$$\tau = c_{cs}(e, \dot{\varepsilon}) + \sigma'\tan(\phi_e) \quad [11]$$

in which $c_{cs}(e, \dot{\varepsilon})$ and ϕ_e are the Hvorslev cohesion and friction angle, respectively; σ' = effective stress; $\sin(\phi_e) = \tan(\alpha_e)$; and $c_{cs}(e, \dot{\varepsilon}) = \frac{a_{cs}(e,\dot{\varepsilon}_a)}{\cos(\phi_e)}$.

There are several important features in Hvorslev failure envelope of [10] or [11] which comprises cohesive and friction components. The Hvorslev surface represents the locus of drained peak strength for heavily overconsolidated clay which also defines stress states at incipient instability signifying the initiation of localized shear band or zone. Sheahan et al. (1996) observed that BBC specimens with high OCRs do exhibit such formation of localized shear bands in CU tests. The cohesive term or component represents the shear strength induced by interparticle forces due to rearrangement of particles at the failure state. This cohesion component is not the true cohesion resulted from adherence between particles at zero confining stress in which no strength is derived from particle rearrangement, sliding friction between particle and particle breakage. The cohesive term is a function of structure or void ratio (or OCR) at the failure, and is a state-dependent parameter. Time-dependent or viscous behaviour of clay under shearing is also attributed to the time-dependent process of particle rearrangement (Soga and Mitchell 2005). Thus, it is postulated that the cohesive term is both state- and rate-dependent. The friction term reflects the shear strength mobilized from sliding between particles at the failure state, and is solely dependent on confining stress as the rate effect on sliding friction is small. The angle α_e or ϕ_e is considered as a material constant, and is lower than the critical state angle α_{cs} or ϕ_{cs}. It may approach the intrinsic friction angle ϕ_μ.

From Fig. 4, the change in OCR due to a change in strain rate at a given consolidation stress, denoted by a change in consolidation pressure Δp_c (distance 'c-d') may be linked to the change in the cohesion intercept Δa_{cs} (distance 'e-f'):

$$[\Delta a_{cs}(e, \dot{\varepsilon}) = K\Delta p_c[\tan(\alpha_{cs}) - \tan(\alpha_e)] \quad [12]$$

$$\Delta c_{cs}(e, \dot{\varepsilon}) = \frac{\Delta a_{cs}(e,\dot{\varepsilon}_a)}{\cos(\phi_e)} \quad [13]$$

where *K* is a factor relating the p-stress at critical state p_{cs} to the maximum consolidation stress p_{cm} ($K = \frac{p_{cs}}{p_{cm}}$) and dependent on the shape of the dynamic yield surface. For critical state model with symmetrical elliptical yield surfaces, $K = \frac{1}{2}$.

The undrained responses of heavily overconsolidated (OC) clay under triaxial compression with varying strain rates are illustrated in a p-q stress plot of Fig. 5. Two clay specimens are allowed to hydrostatically consolidate to a point on a static yield surface (SYS) and rebound to point '1', and sheared undrained at two different strain rates. The undrained stress path of '1-3-4' has a lower strain rate than that '1-5-6'. Both specimens exhibit an undrained peak strength along with strain softening, and fail at different states along CSL. Increase in strain rate results in increase in undrained shear strength, which is similar to those in NC specimens. Thus, the failure behavior of OC specimens at the critical state may be described by [10] or [11].

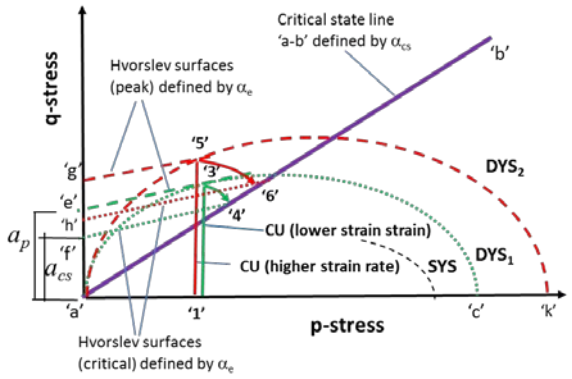

Fig. 5. Undrained behavior of heavily overconsolidated specimens with different strain rates

The undrained peak shear strengths at states '3' and '5' may be expressed using the modified Hvorslev failure envelope (lines 'e-3' and 'g-5' in Fig. 5) by drawing linear effective stress envelope (ESE) passing through these states:

$$q = a_p(e, \dot{\varepsilon}_a) + p\tan(\alpha_e) \quad [14]$$

where $a_p(e, \dot{\varepsilon})$= cohesion intercept depending on void ratio *e* and strain rate $\dot{\varepsilon}$; and the subscript *p* refers to the peak strength state. Equation [14] can be expressed in the conventional Mohr-Coulomb envelope of:

$$\tau = c_p(e, \dot{\varepsilon}) + \sigma'\tan(\phi_e) \quad [15]$$

in which $c_p(e, \dot{\varepsilon})$ = Hvorslev peak cohesion; and $c_p(e, \dot{\varepsilon}) = a_p(e, \dot{\varepsilon})/\cos(\phi_e)$.

In summary, we propose and develop an interpretation technique to incorporate the rate effect on the undrained shear strength measured in CU tests, and to translate the undrained parameters to drained parameters. This effective stress-based technique is founded on Hvorslev postulate on mobilization of cohesion and friction components at failure state. The

cohesion component is rate- and state- dependent whereas the friction component is not.

4 EXPERIMENTAL EVIDENCE (STATE- AND RATE- DEPENDENT UNDRAINED RESPONSE)

To validate and demonstrate the proposed methodology with experimental evidence, a data set reported by Sheahan (1991) and Sheahan et al. (1996) was selected for detailed illustration. They investigated effects of consolidation history, confining stress and strain rate on undrained response of saturated clay in a systematic fashion.

4.1 Material used and test details

The material used is resedimented Boston blue clay (BBC). Among six prepared batches, the average physical properties are: water content = 39.9%, liquid limit = 45.4% and plasticity index = 23.7%. The BBC contains about 48-57% clay sized particles (< 2 μm). The specific gravity is 2.78. The maximum particle size as determined via sedimentation analysis is less than 0.07 mm. The BBC is dominated by illite, illite-smectite, and trioctahedral mica, with lesser amounts of chlorite, hydro-biotite, and kaolinite (Schneider et al. 2011).

The experimental tests include oedometer consolidation tests, CK_0UC tests with varying strain rates, relaxation and creep tests under undrained condition. The data set of twenty five (25) CK_0UC tests is the main interest and focus of this study (Sheahan et al. 1996). Lubricated end platens and a mid-height pore-pressure measurement device were used in the tests to minimize the end friction and pore pressure lag, respectively. Specimens were consolidated to four overconsolidation ratios (OCR) of 1, 2, 4 and 8 with average preshear K_0 values of 0.49, 0.63, 0.84 and 1.11, respectively. The preshear vertical confining pressures varied from 75 to 298 kPa. The undrained shearing was conducted using four axial strain rates of 0.05%, 0.5%, 5%, and 50%/h (1.2, 12, 120 and 1200 %/D). Details of the experimental program and test results can be found in the references aforementioned.

4.2 Test results and interpretation

4.2.1 Undrained Response

For OCR = 1 and 2, BBC exhibits an undrained peak strength with strain softening which is different from with that depicted in Fig. 1b. The undrained peak strength occurs at small axial strain ε of 0.28-0.92%. Strain softening observed after the peak is associated with positive excess pore pressure generation. Increase in OCR causes an increase in peak axial strain ε_{peak} and reduction in strain softening. After the peak, the q-stress decreases continually until reaching the maximum stress obliquity or critical state at large axial strain ε of 14-15% (the maximum stress obliquity defined by q/p ratio where $q = \frac{1}{2}(\sigma'_1 - \sigma'_3)$; $p = \frac{1}{2}(\sigma'_1 + \sigma'_3)$; σ'_1 and σ'_3 are major and minor principal effective stresses, respectively).

For OCR = 4 and 8, the undrained responses are quite different from those for OCR = 1 and 2, but are comparable to those schematically shown in Fig. 1b. The undrained peak strength occurs at axial strain ε_{peak} of 3.7 - 5.2% which are much higher than those observed in low OCR = 1 and 2. In addition, the maximum stress obliquity occurs prior to the undrained peak strength. After the peak, BBC specimens with higher OCR have a higher propensity to dilate under undrained shearing than those specimens with lower OCR. The excess pore pressure generation becomes less severe or even negative, resulting in an increasing mean effective *p*-stress. The ultimate or critical state is attained at large axial strains similar to that observed in low OCR of 1 and 2.

For all OCRs, the undrained strengths mobilized at peak, maximum stress obliquity and ultimate (critical) states are rate-dependent though the dependency decreases with increasing OCR. Increase in strain rate causes increases in the undrained strengths inferring the existence of growing dynamic yield surfaces as illustrated in Figs. 4 and 5. Katti et al. (2003) reanalyzed the test data presented by Sheahan et al. (1996), and showed that the undrained shear strength response and the excess pore pressure response at the peak stress provide quantitatively similar magnitudes of increase in the OCR with increasing strain rate. As strain rate increases, the OCR increases. The apparent change in the OCR is uniquely related to the change in the strain rate which is identical to the isotache rate-dependent (viscous) behaviour observed in 1D constant rate of strain compression tests by Leroueil et al. (1985), and can be considered as an inherent material characteristic.

The OCR also has an effect on failure mode. Diffused shear failure mode was detected in specimens with OCR = 1 whereas distinct shear planes were observed in specimens with OCR = 2, 4 and 8. Due to the localized deformation, the post-peak behaviour of specimens with high OCRs might not be unique.

For a given OCR, the undrained strength increases with increasing strain rate. The increase in undrained shear strength is caused by suppression of shear induced pore pressures Δu_s ($\Delta u_s = \Delta u - (\Delta\sigma_1 + 2\Delta\sigma_3)/3$). For NC clay, the shear induced pore pressure suppression can be explained by time-dependent behavior of the material. At a given deviator stress, the pore pressure generation is larger at slower rates as more creep deformation is allowed under slow loading. The excess pore pressure response is mainly driven by strain in undrained condition. For OC clay, pre-peak behaviour can be explained by the same mechanism in NC clay. After the peak, localized shear deformation produces non-homogeneous pore pressure redistribution which may not reflect overall behavior of the specimen.

It is important to point out that Sheahan et al. (1996) and Katti et al. (2003) did not consider the effect of time-dependent viscous behavior on the undrained shear strength.

4.2.2 Undrained shear strength at ultimate (critical) state

All test specimens reach their ultimate states at axial

strains of about 14-15%. It is reasonable to postulate that the critical state would be attained at such high strains at a given constant void ratio or under undrained condition. Results of ultimate states for all tests were plotted in Fig. 6 to determine the critical state line. Linear regression shows that the best fitted line is characterized with m = 0.491 or ϕ_{cs} = 29.4° with a cohesion of 8.6 kPa (r^2 = 0.989). If the critical state line passes through the origin, then, m = 0.52 or ϕ_{cs} = 31.6° (r^2 = 0.981). The latter will be used as reference line for the analysis. It appears that the effective stress envelope (ESE) of critical state may be considered rate-independent, an intrinsic material property for resedimented BBC. The applied strain rates in CU tests are included in Fig. 6 (some are not shown for clarity). It can be seen that the strength mobilized at the critical state increases with increasing strain rate.

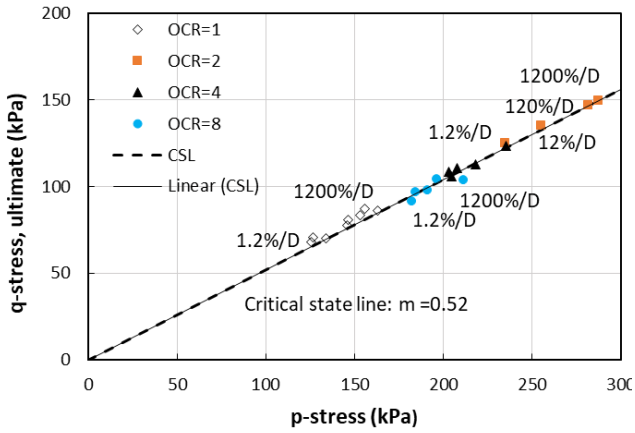

Fig. 6. Shear strength at ultimate state versus mean effective p-stress for CK_0UC tests of OCR = 1, 2, 4 and 8 on resedimented Boston blue clay specimens

The void ratio values at the preshear consolidation were plotted with ultimate p-stresses for all tests to determine the critical state line in an e-p plot (Fig. 7). On the same figure, the NCL is also included. For normally consolidated specimens, the void ratio value varies in a range of 0.77 – 1.02 in confining stresses of 100 - 800 kPa, and the corresponding bulk saturated unit weight lies in a range of 18.4 – 19.4 kN/m^3. Maximum consolidation stresses of about 290 and 585 kPa were applied to specimens with OCR = 1 and OCR = 2 – 8, respectively, explaining the void ratio values shown in Fig. 7. The specimens with OCR =1 have the highest void ratio, followed by specimens with OCR = 8, 4 and 2. The slope values λ for both the critical state and normal consolidation lines are comparable. This parallel feature is consistent with that assumed in the critical state model. The scatter in the critical void ratio values is much larger than that in the critical stress. From Fig. 7, specimens with OCR = 1 are on the 'wet' side of the critical state line, i.e., normally consolidated states. Specimens with OCR = 2 lie close to the critical state line, i.e., lightly overconsolidated states. Specimens with OCR = 4 and 8 are on the 'dry' side of the critical state line showing the evidence of Hvorslev failure surfaces for heavily overconsolidated states.

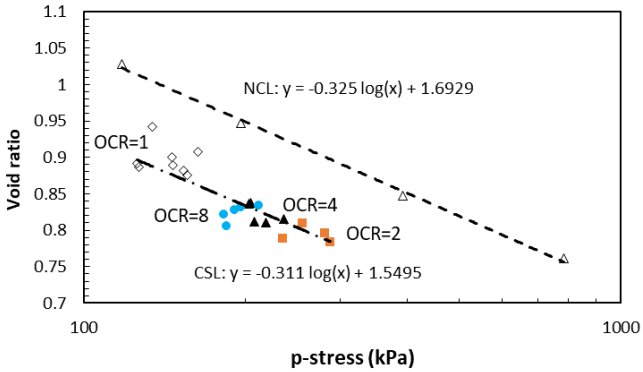

Fig. 7. Final void ratio at critical (ultimate) state versus mean effective p-stress for CK_0UC tests of OCR = 1, 2, 4 and 8 on resedimented Boston blue clay specimens (showing critical state and normally consolidation lines)

4.2.3 Undrained shear strength at peak and maximum stress obliquity states

Results of strengths at peak and maximum obliquity for all undrained tests were presented in p-q plots to show their relative locations with respect to the locus of the critical state line. For clarity, results of tests with low OCR = 1 and 2 and high OCR = 4 and 8 were plotted in Figs. 8 and 9, respectively. Fig. 8 shows that for OCR = 1 and 2 the undrained peak strengths lie well below the critical state line, and increase with strain rate. This behavioral trend substantiates the conceptual undrained response with varying strain rates and existence of evolving DYSs as illustrated in Fig. 4. For OCR = 4 and 8 (Fig. 9), the undrained responses are consistent with those shown in Fig. 5, i.e., the initiation and occurrence of peak strength and maximum stress obliquity are controlled by the shape of the dynamic yield surface. In contrast to the previous two series of OCR = 1 and 2, both the states at the peak strength and maximum stress obliquity lie above the critical state line confirming the existence of the Hvorslev (dynamic) surfaces. In addition, the strains required to mobilize the undrained peak strength in low OCR are much smaller than those in high OCR. The shear resistances or shear deformations derived at the undrained peak strength in low and high OCR are so different that correspondence between two may not be appropriate.

For OCR = 1 and 2, the maximum stress obliquity occurs after the peak strength, and the strains for maximum stress obliquity are large, about 8 – 13 %. For OCR = 4 and 8, the strains for maximum stress obliquity are in general lower than those for peak strength, except in some tests with OCR = 4, and they are within 1 – 5% which are lower than those in tests with OCR = 1 and 2. Thus, the ESE derived from the states at maximum stress obliquity may not reflect the same shear deformation modes in tests with low and high OCRs, which is similar to what happens at undrained peak

strengths.

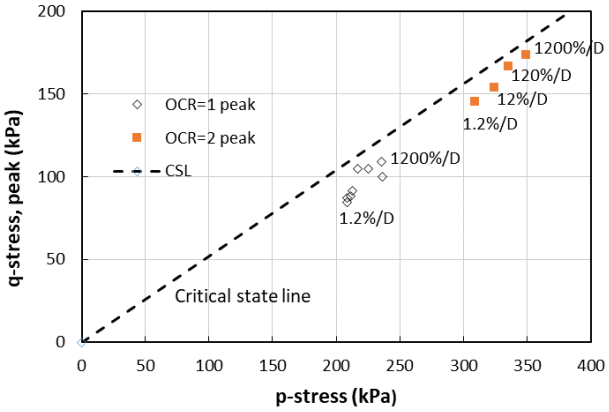

Fig. 8. Shear strength at peak stress versus mean effective p-stress for CK0UC tests of OCR = 1 and 2 on resedimented Boston blue clay specimens

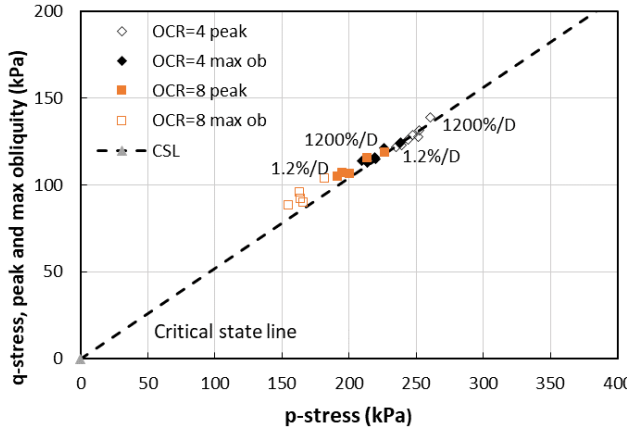

Fig. 9. Shear strength at peak stress and maximum stress obliquity versus mean effective p-stress for CK_0UC tests of OCR = 4 and 8 on resedimented Boston blue clay specimens

5 STATE- AND RATE- DEPENDENT UNDRAINED SHEAR STRENGTH AT CRITICAL STATE

Results of σ'_{vc}-normalized shear strength versus OCR for four different strain rates were plotted in Fig. 10 to determine the S and m parameters in [4]. Then, the values of S parameter were plotted against strain rates in Fig. 11, and the linear regression relationship was substituted into [9]. Using an average value of m parameter (m = 0.65), [9] was used to predict state- and rate- dependent undrained shear strength of BBC. Fig. 12 compares results from the CU tests and the model. The trends substantiate the postulate made in [8]. The rate effect on the undrained shear strength increases with increasing OCR.

The above exercise could be applied to investigate the behavior of heavily OC BBC specimens at the undrained peak state. However, there is not sufficient data for regression analysis as only two data sets of CU tests with OCR = 4 and 8 are available.

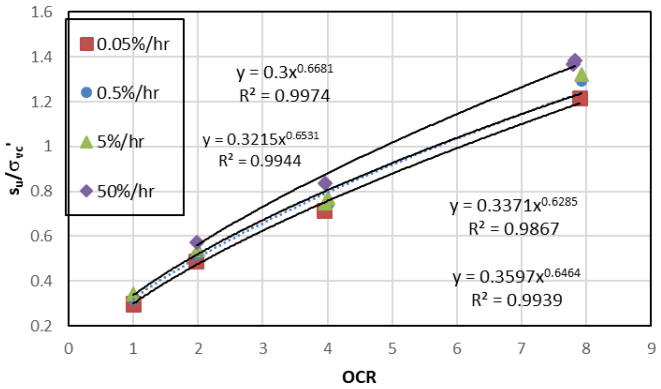

Fig. 10. Experimental data of σ'_{vc}-normalized undrained shear strength at critical state versus OCR for CK_0UC tests of OCR = 1, 2, 4 and 8 on resedimented Boston blue clay specimens (Sheahan et al. 1996). Power laws of [4] are used to curve fit the data

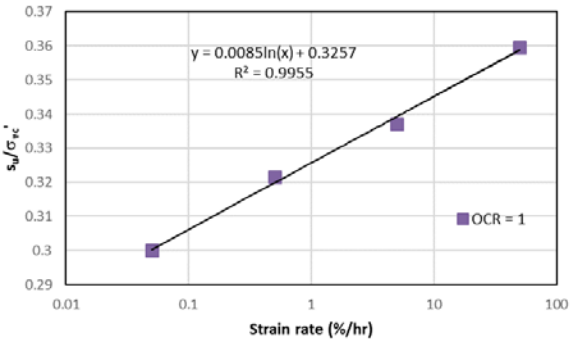

Fig. 11. Experimental data of σ'_{vc}-normalized undrained shear strength at critical state versus strain rate for CK_0UC tests of OCR = 1 on resedimented Boston blue clay specimens (Sheahan et al. 1996). Semi-logarithmic law is used to curve fit the data

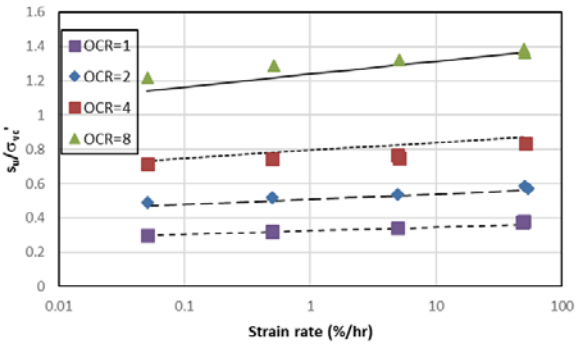

Fig. 12. Comparison between experimental data and predicted results of σ'_{vc}-normalized undrained shear

strength at critical state versus strain rate for CK_0UC tests of OCR = 1-8 on resedimented Boston blue clay specimens (Sheahan et al. 1996). Semi-logarithmic lower law is used to curve fit the data

6 STATE- AND RATE- DEPENDENT COHESION AND INTRINSIC FRICTION ANGLE AT CRITICAL STATE

Determination of the rate-dependent cohesion of BBC from [11] requires the value of Hvorslev friction angle. The value of Hvorslev friction angle was not reported by Sheahan et al. (1996). The composition of BBC is dominated by illite. de La Beaumelle (1991) reported a peak angle of 22.5º for natural BBC based on direct shear and triaxial compression tests. Tembe et al. (2010) reported a binary mixture (50-50%) of illite and quartz yields a friction coefficient of 0.439 or equivalent angle of 21º. It is reasonable to assume the ϕ_e for BBC lies in a narrow range of 21-22.5º.

With ϕ_e = 21º, Hvorslev cohesion values at critical states ($c_{cs}(e,\dot{\varepsilon})$) for tests with OCR = 1, 2 , 4 and 8 were calculated at varying strain rates using [11], respectively. The results were normalized with the vertical consolidation stress, and plotted in Fig. 13, along with semi-logarithmic correlations. From this figure, it is clear that cohesion is rate-dependent, and the dependency increases with OCR.

Hvorslev cohesion values calculated from results of tests with OCR = 1, 2, 4 and 8 were plotted against void ratio in Fig. 14. This figure clearly illustrates that the cohesion increases with decreasing void ratio. As the void ratio depends on consolidation history, it implies that the cohesion is function of consolidation history. From Fig. 14 in which the test data were grouped according to the strain rate range, the results show a trend of cohesion increasing with increasing strain rate. It appears that the cohesion is less sensitive to change in strain rate than that in void ratio. The plots of Fig. 14 provide unique interrelationships among cohesion, strain rate and void ratio of BBC, which can be considered as intrinsic material properties. Using the least square method, the following correlation among the void ratio, strain rate and Hvorslev cohesion is obtained for given ϕ_e = 21º:

$$c_e = -168.58e + 1.289\log(\dot{\varepsilon}) + 178 \quad [16]$$

where c_e and $\dot{\varepsilon}$ are in kPa and %/D, respectively.

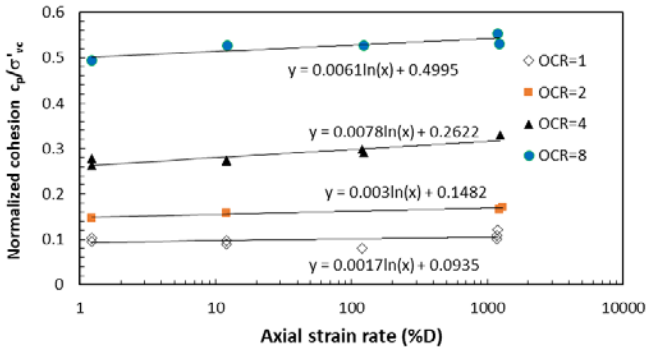

Fig. 13. Normalized cohesion versus axial strain rate for CK_0UC tests of OCR = 1, 2, 4 and 8 on resedimented Boston blue clay specimens

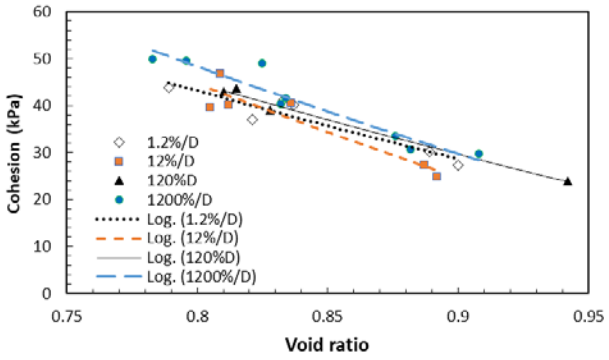

Fig. 14. Experimental results of CK_0UC tests on resedimented Boston blue clay specimens – (a) cohesion versus void ratio for varying OCR, and (b) cohesion versus void ratio for varying strain rates

7 CONCLUDING REMARKS

This paper develops a methodology to determine rate-dependent effective-stress parameters from responses of cohesive soils in consolidated undrained triaxial compression tests with varying strain rates. Increase in strain rate results in an apparent increase in OCR, and thus the size of the dynamic yield surface (DYS). The DYSs on the 'dry' and 'wet sides of the critical state are unsymmetrical producing peak strengths above and below the critical state, respectively. The failure states on the critical state line are represented by Hvorslev strength components consisting of void ratio- and rate-dependent cohesion and intrinsic rate-independent friction angle. Increase in strain rate causes increase in cohesion. This cohesion is not the same as those derived from interparticle or cementing bonds. The rate-dependent strength parameter should be used in design and analysis of practical problems in which the effect of loading rate on the behaviour of the engineered system is critical, such as buried pipelines in moving slopes.

ACKNOWLEDGEMENTS

The authors appreciate the support provided by the

Natural Science and Engineering Council of Canada (NSERC) and University of Calgary. Experimental data used in this work are from publications and doctoral dissertation of Dr. Thomas C. Sheahan.

REFERENCES

Budhu, M. 2011. Soil mechanics and foundations. 3rd edition. John Wiley & Sons, Inc. 761 pages.

Casagrande, A., and Wilson, S.D. 1951. Effect of rate of loading on the strength of clays and shales at constant water content. *Geotechnique,* 2(3): 251–263.

de La Beaumelle, A.C.L.A. 1991. Evaluation of SHANSEP strength-deformation properties of undisturbed Boston blue clay from automated triaxial testing. M.Sc. Thesis, Massachusetts Institute of Technology.

Graham, J., Crooks, J.H.A. and Bell, A.L. 1983. Time effects on the stress-strain behavior of natural soft clays. *Geotechnique,* 33(3): 327-340.

Katti, D.R., Tang, J. and S. Yazdani, S. 2003. Undrained response of clays to varying strain rate. *J. Geotech. Geoenviron. Eng*., 2003, 129(3): 278-282.

Kulhawy, F.H. and Mayne, P.W. 1990. Manual on estimating soil properties for foundation design. Final Report, Project 1493-6, EL-6800, Electric Power Institute, Palo Alto, CA.

Kutter, B.L. and Sathialingam, N. 1992. Elasticviscoplastic modelling of the rate-dependent behaviour of clays. *Geotechnique,* 42(3): 427-441.

Ladd, C. C. and Foot. R. 1974. New design procedure for stability of soft clays. *J. Geotech. Eng. Div.* ASCE, 100(7): 763 - 786.

Lefebvre, G. and Pfendler, P. 1996. Strain rate and preshear effects in cyclic resistance of soft clay. *J. Geotech. Eng.,* 122(1): 21–26.

Leroueil, S., Kabbaj, M., Tavenas, F. and Bouchard, R. 1985. Stress-strain-strain rate relation for the compressibility of sensitive natural clays. *Geotechnique*, 35(2): 159-180.

Mayne, P.W. 1980. Cam-clay prediction of undrained strength. *J. Geotech. Eng. Division,* 106(GT11): 1219-1242.

Nakai, T., Shahin, H.M., Kikumoto, M., Kyokawa, H., Zhang, F. and Farias, M.M. 2011. A simple and unified three-dimensional model to describe various characteristics of soils. *Soils and Foundations,* 51 (6): 1149–1168.

Perzyna, P. 1963. The constitutive equations for rate sensitive plastic materials. *Quarterly of Applied Mathematics*, 20(4): 321-332.

Richardson, A.M. and Whitman, R.V. 1963. Effect of strain-rate upon undrained shear resistance of a saturated remoulded fat clay. *Geotechnique*, 13(3): 310-324.

Sheahan, T.C. 1991. An experimental study of the time-dependent undrained shear behavior of resedimented clay using automated stress path triaxial equipment. PhD dissertation, Massachusetts Institute of Technology, Mass.

Sheahan, T.C. 1995. “nterpretation of undrained creep tests in terms of effective stresses. *Canadian Geotechnical Journal,* 32: 373-379.

Sheahan, T.C., Ladd, C.C., and Germaine, J.T. 1996. Rate-dependent undrained shear behavior of saturated clay. *J. Geotech. Eng.,* 122(2): 99–108.

Soga, K. and Mitchell, J.K. 1996. Rate dependent deformation of structured natural clays. *Proc. Am. Soc. Civ. Eng.,* Geotech. Special Publication No. 61, pp. 243–257.

Soga, K. and Mitchell, J.K. 2005. Fundamentals of soil behavior. Third edition, John Wiley & Sons Inc.

Schneider, J., Flemings, P.B., Day-Stirrat, R.J. and Germaine, J.T. 2011. Insights into pore-scale controls on mudstone permeability through resedimentation experiments. *Geology*, 39: 1011-1014.

Taylor, D.W. 1943. Cylindrical compression research program on stress-deformation and strength characteristics of soils. *9th Progress Report*, U.S. Army Corps. of Engineers, Waterways Expt. Station, MIT, Mass.

Tembe, S., Lockner. D.A. and Wong. T-F. 2010). Effect of clay content and mineralogy on frictional sliding behavior of simulated gouges: Binary and ternary mixtures of quartz, illite, and montmorillonite.” *Journal of Geophysical Research: Solid Earth*, Volume 115, Issue B3. https://doi.org/10.1029/2009JB006383.

Vaid, Y.P., and Campanella, R.G. 1977. Time-dependent behavior of undisturbed clay. *ASCE Journal of the Geotech. Eng. Division*, 103(7): 693-709.

Wong, C.K., Wan, R.G., and Wong, R.C.K. 2018. A methodology for estimating creep deformation from consolidation deformation in 1D compression. *ASCE International Journal of Geomechanics*, 18(6). https://doi.org/10.1061/(ASCE)GM.1943-5622.0001162.

Wroth, C.P. 1984. The interpretation of in situ soil tests. *Geotechnique*, 34(4): 449-489.

Zhu, J., and Yin J-H. 2000. Strain-rate-dependent stress-strain behavior of overconsolidated Hong Kong marine clay. *Canadian Geotechnical Journal*, 37(6): 1272-12.